Do great earthquakes occur on the Alpine fault in central South Island, New Zealand?

R. Sutherland[1], D. Eberhart-Phillips[2], R.A. Harris[3], T. Stern[4], J. Beavan[1], S. Ellis[1], S. Henrys[1], S. Cox[2], R.J. Norris[5], K.R. Berryman[1], J. Townend[4], S. Bannister[1], J. Pettinga[6], B. Leitner[1], L. Wallace[1], T.A. Little[4], A.F. Cooper[5], M. Yetton[7], M. Stirling[1].

1. GNS Science, 1 Fairway Drive, PO Box 30-368, Lower Hutt, NZ.
2. GNS Science, Private Bag 1930, Dunedin, NZ.
3. U.S. Geological Survey, Menlo Park, CA 94025-3591, USA.
4. Victoria University of Wellington, PO Box 600, Wellington, NZ.
5. University of Otago, PO Box 56, Dunedin, NZ.
6. University of Canterbury, Private Bag 4800, Christchurch 8020, NZ.
7. Geotech Consulting, RD1 Charteris Bay, Lyttelton R.D., NZ.

Corresponding author: Rupert Sutherland
Email: r.sutherland@gns.cri.nz; Tel: (+NZ) 4 570 4873
Submitted for publication in AGU Geophysical Monograph, SIGHT project
Keywords: Alpine fault; earthquakes; strike-slip faults; seismic slip; tectonics; transpression

ABSTRACT

Geological observations require that episodic slip on the Alpine fault averages to a long-term displacement rate of 2-3 cm/yr. Patterns of seismicity and geodetic strain suggest the fault is locked above a depth of 6-12 km and will probably fail during an earthquake. High pore-fluid pressures in the deeper fault zone are inferred from low seismic P-wave velocity and high electrical conductivity in central South Island, and may limit the seismogenic zone east of the Alpine fault to depths as shallow as 6 km. A simplified dynamic rupture model suggests an episode of aseismic slip at depth may not inhibit later propagation of a fully developed earthquake rupture. Although it is difficult to resolve surface displacement during an ancient earthquake from displacements that occurred in the months and years that immediately surround the event, sufficient data exist to evaluate the extent of the last three Alpine fault ruptures: the 1717 AD event is inferred to have ruptured a 300-500 km length of fault; the 1620 AD event ruptured 200-300 km; and the 1430 AD event ruptured 350-600 km. The geologically estimated moment magnitudes are 7.9 ± 0.3, 7.6 ± 0.3, and 7.9 ± 0.4, respectively. We conclude that large earthquakes (M_w >7) on the Alpine fault will almost certainly occur in future, and it is realistic to expect some great earthquakes (M_w ≥8).

INTRODUCTION

The Alpine fault is a mature dextral strike-slip fault that offsets basement rocks by ~470 km and offsets deposits of the last glaciation (18-80 ka) by 0.4-2.0 km [*Wellman and Willett*, 1942; *Wellman*, 1953; *Norris and Cooper*, 2001; *Sutherland et al.*, 2006]. The surface trace is continuous for at least 800 km (Fig. 1), and has no separations of >5 km [*Wellman and Willett*, 1942; *Norris et al.*, 1990; *Berryman et al.*, 1992; *Barnes et al.*, 2005]. In central South Island, the fault is locally transpressive and the surface trace bounds the western edge of the mountains [*Norris et al.*, 1990]. Although the Alpine fault is identified as a laterally continuous crustal structure with an average late Quaternary surface displacement rate of 2-3 cm/yr [*Berryman et al.*, 1992; *Norris and*

Cooper, 2001; *Sutherland et al.*, 2006], there have been no large earthquakes causing surface rupture on the fault since European settlement in ca. 1800 AD. Since a national seismic network was installed and continuously improved (during the last 50 years), it has also become clear that small and moderate-sized earthquakes are less frequent near the Alpine fault in central South Island than at any other part of the plate boundary through New Zealand [*Evison*, 1971; *Eberhart-Phillips*, 1995]. The lack of moderate or large-magnitude earthquakes on the Alpine fault since reliable record keeping started means that the seismic potential of the Alpine fault must be inferred from indirect observations and theoretical considerations.

It has been argued that high heat-flow and a shallow brittle-ductile transition make it physically unlikely that elastic strains of sufficient size could accumulate to generate great earthquakes and that the measured geodetic strains can be explained if a significant proportion of plate boundary displacement is accommodated aseismically [*Walcott*, 1978; *Walcott*, 1998]. Moreover, an extensive region of low seismic wave speeds [*Smith et al.*, 1995; *Stern et al.*, 2001; *Eberhart-Phillips and Bannister*, 2002] and high electrical conductivity [*Wannamaker et al.*, 2002] within the Alpine fault zone suggests that high fluid pressures may be present, and supports the hypothesis that the Alpine fault is not able to sustain high shear stresses. This raises several key questions. Could some component of long-term displacement on the Alpine fault be accommodated by mechanisms other than large earthquakes [*Stern et al.*, 2001]? Continental strike-slip faults of similar dimensions to the Alpine fault typically fail in large earthquakes [*Wells and Coppersmith*, 1994; *Hanks and Bakun*, 2002; *Lin et al.*, 2002; *Eberhart-Phillips et al.*, 2003], but is the Alpine fault atypical? Is it possible that some component of long-term Alpine fault slip may be accommodated by slow ruptures, afterslip or during a succession of smaller earthquakes? Even if the Alpine fault does fail in large earthquakes, then it may not exclusively rupture in large earthquakes in every seismic cycle; by analogy, the Santa Cruz section of the San Andreas fault ruptured in earthquakes of different magnitude in 1906 and 1989.

One objective of the SIGHT project, and related projects, was to better determine Alpine fault geometry and physical properties at depth, so that its seismic potential in central South Island could be better understood. We review and synthesise the data that are now available and present new modeling to address what the seismic potential of the Alpine fault might be. Does the Alpine fault fail in large (M_w >7) earthquakes? Does the Alpine fault fail in great (M_w ~8) earthquakes? We explore these questions and, in the light of our conclusions, make recommendations for future data collection activities that could underpin improved quantitative seismic hazard models for central South Island.

SURFACE EXPRESSION

The Alpine fault varies significantly in character along its length (Fig. 1). From its southern termination near the Puysegur subduction thrust to offshore from Caswell Sound, the Alpine fault scarp is up-to-the-northwest in most places and the trace is segmented into a series of right-stepping sections, small pull-apart basins, and minor transpressional ridges [*Barnes et al.*, 2001; *Barnes et al.*, 2005]. At Caswell Sound a right step in the fault trace of about 5 km occurs [*Barnes et al.*, 2005]. From Caswell Sound to the Cascade River (Fig. 1), surface trace continuity is disrupted by minor (<200 m) step-overs and the scarp is up-to-the-northwest offshore and at most localities onshore. Slickensides and offset topography constrain the average surface slip vector onshore between Milford Sound and Cascade River to plunge at <5° [*Berryman et al.*, 1992; *Sutherland and Norris*, 1995; *Barnes et al.*, 2005; *Sutherland et al.*, 2006].

A zone of overlapping fault traces about 1 km wide near Cascade River is accompanied by a change in character of the fault trace. North of Cascade River to Haast River (Fig. 1), the fault trace becomes up-to-the-southeast, but the displacement is still primarily dextral strike-slip and the fault trace remains about two kilometres northwest of the range front [*Berryman et al.*, 1992; *Cooper and Norris*, 1995]. The c. 7° clockwise change in regional strike of the fault trace north of Cascade River should reduce the convergent component of plate motion across the fault, but reverse movement in fact becomes more pronounced; this observation suggests that regional changes in geology either side of the fault play a significant role in determining the nature of slip partitioning at the plate boundary.

North of Haast River to Taramakau River (Fig. 1), the Alpine fault trace lies at the rangefront and is segmented at a scale of 1-5 km into a series of strike-slip and moderately southeast-dipping oblique-thrust sections [*Norris et al.*, 1990; *Berryman et al.*, 1992]; thrust sections are often difficult to recognise on air photos or in the field, except where river exposures reveal cataclasite thrust over Quaternary sediments.

Between Taramakau River and Lake Rotoiti (Fig. 1), the Alpine fault surface trace is up-to-the-southeast and lies near to the range front [*Berryman et al.*, 1992; *Nathan et al.*, 2002]. Near Taramakau River, the Alpine fault and Hope fault intersect at an acute angle. There is a substantial restraining bend in the Alpine fault southwest of Lake Rotoiti, where the Awatere fault merges with the Alpine fault. Northeast of Lake Rotoiti, the Alpine fault is continuous with and becomes reclassified as the Wairau fault.

SURFACE DISPLACEMENT RATE

The Alpine fault surface displacement rate in the region between Milford Sound and Cascade River is 23 ± 2 mm/yr (95% confidence), as determined from multiple measured offsets that accumulated over a time interval of 18-79 kyr [*Sutherland et al.*, 2006]. The very similar character of the offshore Milford-Caswell section with that onshore, and a glacial moraine offset by a similar magnitude to those onshore, suggest that a similar displacement rate continues at least as far south as Caswell Sound [*Barnes et al.*, 2005]. The prominent surface trace and rapid rates of deformation in adjacent basins suggests that there is also a rapid (1-3 cm/yr) displacement rate south of Caswell Sound [*Barnes et al.*, 2001].

At Haast River, the surface strike-slip displacement rate is determined to be >21 mm/yr from an offset terrace of age <4.4 cal ka [*Cooper and Norris*, 1995] and 28 ± 4 mm/yr from a terrace surface offset 25 m since 0.74 cal ka [*Berryman et al.*, 1998]. Between Haast River and Taramakau River, numerous exposures of a discrete fault zone emplacing shattered mylonite over Quaternary sediments suggest rapid rates of Quaternary displacement; this is confirmed by estimates of strike-slip displacement rate of 27 ± 5 mm/yr [*Norris and Cooper*, 1997], >22 mm/yr [*Cooper and Norris*, 1994], and 29 ± 6 mm/yr [*Wright*, 1998], and estimated dip-slip displacement rates of 7.8 ± 1, >6.7, 6 ± 1, >12, 8 ± 3, and 7.5 ± 1.5 mm/yr [*Norris and Cooper*, 2001].

Northeast of Taramakau River, where there exists a zone of intersection with the Hope fault, the Alpine fault displacement rate is determined to be ≥6.3 ± 2 mm/yr [*Yetton et al.*, 1998] and 10 ± 2 mm/yr [*Berryman et al.*, 1992]. The Alpine fault displacement rate diminishes to the northeast, as the intersection with the Awatere fault is passed, and is estimated to be 4 ± 1 mm/yr where the Alpine fault is reclassified as the Wairau fault [*Berryman et al.*, 1992; *Zachariasen et al.*, 2006].

EVIDENCE FOR ALPINE FAULT CREEP AT THE SURFACE

It has previously been suggested that shallow aseismic deformation may be occurring near or on the Alpine fault in central South Island [*Walcott*, 1978; *Walcott*, 1998]. Trenching, natural exposures, and geomorphic offsets indicate that long-term displacement on the shallowest part of the Alpine fault (<1 km depth) is localised in a narrow zone and has a rate of 2-3 cm/yr, when averaged over >1000 yr [*Norris and Cooper*, 2001].

The most famous experiment to investigate the existence of Alpine fault creep was the construction (under the supervision of F. Evison) in 1964 of a concrete monitoring wall near Springs Junction (Fig. 1), which is north of the Alpine-Hope fault intersection [*Beanland*, 1987]. The "Evison wall" and sealed roads in ten locations are built across the Alpine fault, but show no signs of deformation over a period of >40 yr. Other man-made structures that cross the Alpine fault include delicate infrastructure items such as a petrol station at Franz Josef and several water races and tunnels associated with the Dilmans Hydroelectric scheme near Taramakau river (Fig. 1), where even a very small displacement is likely to have been noticed. No such displacement has been reported.

In addition to human features, several natural river terraces that are >40 years old cross the Alpine fault in central South Island, but show no sign of deformation, even though a clear scarp exists on older terraces [*Adams*, 1980]. This observation is supported by trenches and exposures, where undeformed sediment is observed overlying faulted sediment [*Yetton et al.*, 1998].

If Alpine fault creep had occurred during the decades in which geodetic observations have been made, then higher strain rates would be expected on small-aperture survey networks that span the Alpine fault, as compared to larger-aperture networks. However, no significant difference is observed between networks with apertures of 1-5 km [*Wood and Blick*, 1986] and networks with apertures of c. 30 km [*Walcott*, 1979; *Beavan et al.*, 1999].

By analogy with the creeping section of the San Andreas fault, spatial clustering of small-magnitude earthquakes would be expected close to the Alpine fault, if it were creeping near the surface. This is not observed [*Eberhart-Phillips*, 1995].

It is very difficult to rule out the possibility that some aseismic deformation may be occurring in the mountainous region immediately east of the Alpine fault trace, but the evidence described above precludes significant creep on the surface part of the Alpine fault during the last 40 yr and strongly suggests that none has occurred in >100 yr.

HISTORICAL SEISMICITY

Seismicity is distributed in a broad region near the Alpine fault and extending approximately 100 km to the southeast. Moderate magnitude earthquakes (M_w >5.0) recorded from 1928-1999 have occurred in the vicinity of the Alpine fault, but these historic epicentres are more poorly determined: it is not possible to say if they represent Alpine fault events.

The stress field near the Alpine fault was computed after the SAPSE experiment from focal mechanisms: the regional stress field has a subhorizontal axis of maximum compressive stress that trends 110–120º [*Leitner et al.*, 2001], a direction similar to the azimuth of maximum contractional strain rate [*Beavan et al.*, 1999] and at an angle that is ca. 60° oblique to the strike of the Alpine fault. At 80% confidence level, stress tensors for all regions in the Southern Alps are the same [*Leitner et al.*, 2001].

The maximum depth of seismicity provides an estimate of the thickness of the seismogenic zone and, therefore, relates to the depth of the brittle-ductile transition zone [*Scholz*, 2002]. The maximum depth of crustal seismicity is uniform over large parts of

central South Island at ~12 km. The SAPSE experiment recorded 60 earthquakes in a swath extending from 5 km northwest to 15 km southeast of the surface trace of the Alpine fault [*Leitner et al.*, 2001]. Given an approximate fault dip of 45°, these earthquakes occurred on or close to the fault, delineating its seismogenic zone. Seismicity was highest just north of Milford Sound. In central South Island (near Franz Josef), seismicity near the Alpine fault was low during the SAPSE experiment and during the 8 years of New Zealand national seismic network (NZNSN) recordings. However, the occurrence of a few earthquakes with hypocentral depths of as much as 10 km suggests that crust in the vicinity of the Alpine fault is capable of storing and then releasing elastic strain.

When similar magnitude ranges are considered, the seismicity rate of the Alpine fault is comparable with seismicity rates along locked sections of the San Andreas fault [*Leitner et al.*, 2001]. The moment release rate, calculated from NZNSN seismicity between 1990 and 1997 across the region, is highest at the Alpine fault, decreases toward the east, and shows another small maximum at 75-95 km distance from the Alpine fault. The distribution of moment release rate across the Southern Alps has a similar pattern to model strain rates [*Koons et al.*, 1994; *Koons et al.*, 1998] and measured strain rates [*Beavan et al.*, 1999; *Wallace et al.*, submitted], but is 2-3 orders of magnitude smaller than predicted if all the plate convergence had been accommodated by earthquakes during that period. Only a small fraction of the plate boundary strain that accumulated during the last 150 years has been released during earthquakes.

EVIDENCE FOR ANCIENT ALPINE FAULT EARTHQUAKES

Direct earthquake indicators

Pseudotachylyte, which is interpreted to be quenched melt generated by friction during seismic slip, is well documented within fault rocks of the Alpine fault zone in central South Island [*Reed*, 1964; *Wallace*, 1976; *Sibson et al.*, 1979; *Bossiere*, 1991; *Warr and van der Pluijm*, 2005]. The direct association of friction melts with fault rocks of the Alpine fault supports the hypothesis that seismic slip occurs on the Alpine fault, but places little constraint on the magnitude of seismic events.

Trenches across the Alpine fault near Haast and Okuru (Fig. 1) show extensive evidence for liquefaction of sand layers, sand dykes, and sand extrusion onto paleosols [*Berryman et al.*, 1998]. The evidence for extensive liquefaction is consistent with shaking of intensity MM>7. The coincidence of sand extrusion horizons with the bases of colluvial wedges adjacent to the fault scarp suggests a causal relationship between liquefaction and fault scarp formation. Liquefaction of sand adjacent to the Alpine fault scarp is also reported from a trench (Kokatahi-2) 20 km southwest of Taramakau River [*Yetton*, 1998; *Yetton et al.*, 1998].

Episodic scarp formation

In the Haast-Okuru-Turnbull region, five trenches across faulted fluvial terraces show clear evidence for episodic surface rupture [*Berryman et al.*, 1998]. Fault surfaces that are overlain by undeformed sediment layers indicate tectonic quiescence after the last movement at each fault location. Intercalation of colluvial wedges and paleosols on the downthrown side of the scarp indicate episodic scarp formation, followed by scarp degradation, and subsequent soil formation. The correspondence of the base of the colluvial wedges with strata containing sand extruded from liquefaction features, and the upper truncation surfaces of faults, strongly suggests a causal relationship between episodic scarp formation, faulting, and strong shaking. Radiocarbon dating of the three

'event horizons' limits the timing of the three most recent earthquakes in the Haast region to 700-800 AD, 1160-1410 AD, and post 1480 AD. Surface displacement of 25 m is measured from offset river channels on terrace surfaces at the Haast and Okuru sites, and hence it is inferred that the horizontal surface offset during each faulting event was 8-9 m, with about 1 m of vertical motion. Additional evidence for horizontal surface faulting of 8-9 m during each of the last two fault movement events comes from offset river channels at Hokuri Creek [*Hull and Berryman*, 1986; *Sutherland and Norris*, 1995].

Fault scarps along the Alpine fault between Haast River and Toaroha River have not been excavated for paleoseismic investigations. However, evidence for discrete uplift events comes from a flight of terraces adjacent to the Karangarua River (Fig. 1) immediately upstream from the Alpine fault [*Adams*, 1980]. Based on the age of forest cover determined by cores in tree trunks, the youngest terrace that no longer floods was abandoned in 1710-1720 AD, the next highest terrace was abandoned in 1600-1620 AD, and the terrace above that was abandoned in 1405-1445 AD [*Yetton et al.*, 1998].

In the region between Ahaura River and Toaroha River, truncated fault planes in six trenches and variably-deformed or undeformed scarp collapse deposits provide evidence for two discrete faulting events during the last 500 years [*Yetton*, 1998; *Yetton et al.*, 1998]. Radiocarbon data indicate that the earlier event occurred at 1480-1645 AD and the most recent event occurred after 1660 AD, and probably during 1700-1750 AD [*Yetton*, 1998; *Yetton et al.*, 1998]. Trenching evidence shows that the most recent event ruptured the Alpine fault up to 25 km northeast of its intersection with the Hope fault .

Paleoseismic trenching between Ahaura River and Lake Rotoiti demonstrates that the most recent event along the northern section of the Alpine fault (1480 – 1645 AD) appears to correspond with the penultimate event (c. 1620 AD) recognised in the more southern trenches [*Yetton*, 2002]. Paleoseismic trenching of the Wairau fault suggests it has not ruptured during the last c. 2000 yr [*Zachariasen et al.*, 2006].

Age of forest damage and landslides

Evidence for vegetation damage comes from: the age of dead trees, the age of regenerating forest in areas that have undergone a significant disturbance, and tree-ring evidence from mature living trees that have survived a significant period of growth disturbance. Forest damage close to the Alpine fault was reported on the north side of Milford Sound, where trees had lost their crowns; the forest damage event was dated by tree trunk circumference to have been during the period 1650-1725 AD [*Cooper and Norris*, 1990].

Regional studies of forest dynamics and tree growth suppression have revealed significant forest disturbance events at 1700-1730 AD, 1610-1640 AD, and 1410-1440 AD [*Wells et al.*, 1998; *Yetton et al.*, 1998; *Wells et al.*, 1999; *Wells et al.*, 2001; *Cullen et al.*, 2003]. Widespread slope instability during these forest disturbance events is implied by large stands of forest that have no trees older than a certain age and that are substantially younger than the maximum life expectancy of mature species [*Wells et al.*, 1998]. The most recent forest disturbance event is inferred to correlate with a significant growth suppression event recorded by cross-matched tree ring analysis to have occurred in 1717 AD [*Wells et al.*, 1999]. Another significant growth suppression event is recorded from the Waitaha River region at c. 1620 AD [*Wright*, 1998].

Another study that investigated the rockfall and landslide history of the Southern Alps utilised the distribution of lichen sizes on exposed boulders; clusters in lichen size were used to infer intense regional shaking at 1738-1758 AD, 1479-1499 AD, and 1216-1236 AD [*Bull*, 1996]. The 1748 AD age is slightly older (33 ± 18 yr) and barely

resolved from the 1700-1730 age of forest disturbance. The 1489 AD age is 64 ± 18 yr older than the 1410-1440 age of forest disturbance. Uncertainties in both approaches may be larger than the quoted formal errors, and so it could be that the true ages cluster after the two largest recent Alpine fault earthquakes. However, some caution must be applied when interpreting the lichen data, because the closest site to the Alpine fault is 18 km away, and most sites are >25 km distant. It is possible that the lichen study dates rockfall deposits that were caused by earthquakes in the central Southern Alps, rather than on the Alpine fault.

A reappraisal of radiocarbon age clustering

It has been suggested on the basis of radiocarbon dating of aggradation and mass-movement deposits younger than 1250 AD, that these deposits have ages that cluster at times around, or shortly after the times of substantial forest disturbance [*Adams*, 1980; *Yetton*, 1998; *Yetton et al.*, 1998]. We reconsider the statistical question of how significant the clustering of the 19 reported radiocarbon ages is, in the light of recent advances in calibration of the radiocarbon timescale (Fig. 2).

We assume a null hypothesis that the true age of the wood samples is equally frequent during the period 1300-1750 AD. The oldest bracketing age was chosen on the basis of the calibrated ages of the oldest radicarbon-dated samples. The youngest bracketing age was chosen to be slightly younger than the youngest period of substantial forest disturbance [*Wells et al.*, 1998; *Wells et al.*, 1999]. A model frequency distribution of radiocarbon ages was computed from the southern hemisphere calibration dataset [*McCormac et al.*, 2004], assuming a typical radiocarbon error of 50 ^{14}C yr, and then the data were compared with the model (Fig. 2).

Although independent evidence provided by the forest disturbance ages do imply distinct episodes of enhanced mass-movement and aggradation, and these are a good match to radiocarbon ages of event horizons in paleoseismic trenches, it is apparent from Figure 2 that the random model (null hypothesis) and observed frequency distributions for radiocarbon ages of aggradation and mass movement deposits are remarkably similar: the model peaks at 1700-1730 AD and 1610-1640 AD can be explained entirely from the distribution of radiocarbon ages within the calibration dataset, whereas a low frequency is predicted for the 1410-1440 AD period. We conclude that there is no definitive radiocarbon evidence for an increased frequency of aggradation events at either 1700-1730 AD or 1610-1640 AD. The observed frequency for the 1410-1440 AD event is nearly double the predicted frequency, but there are only five relevant samples and two of those are associated with the same (Toaroha river) terrace sequence. Although it is reasonable to suggest that times of enhanced mass-movement and terrace aggradation accompany earthquake events, we conclude that the existing mass movement and aggradation radiocarbon dataset is too small, and the ages too imprecise, to determine if there are significant clusters in the ages of mass movement and aggradation deposits.

ALPINE FAULT GEOMETRY AND PHYSICAL PROPERTIES AT DEPTH

Seismic reflection data have revealed reflectors associated with the Alpine fault zone at depth. Reflections with 9-15 s two-way-travel-time and reverse moveout were recorded east of the Alpine fault [*Davey et al.*, 1995; *Kleffman et al.*, 1998]; these reflections define a boundary, 20-30 km deep, dipping southeast at 40-60°, that, when projected to the surface, coincides with the surface trace of the Alpine fault. Stacked images reveal a bright reflective zone that can be traced from the mid-crust into a broad,

sub-horizontal zone of diffuse, but strong, reflectivity at a depth of about 30 km [*Okaya et al.*, 2002].

Anomalous time delays on seismographs west of the Alpine fault were first reported after an experiment in 1995 that used large dynamite shots offshore of the east coast of South Island [*Smith et al.*, 1995]; the travel-time delays were consistent with a low-seismic-velocity region deep within the hanging wall of the Alpine fault. This preliminary model was tested with a higher resolution survey in 1998 [*Stern et al.*, 2001]: time delays from a series of 50-100 kg dynamite shots from the McKenzie basin were recorded on a 60 channel seismic array located in the lower part of the Karangarua river valley, just 6 km east of the Alpine fault. Maximum delays of 0.8 s were recorded. These data, in conjunction with observations of teleseismic P-wave delays permitted a roughly elliptical zone of low P-wave speeds to be delineated. The dimensions of the low-seismic-wave-speed zone are approximately 40 km by 25 km and the P-wave speed is 6-10% less than surrounding regions [*Stern et al.*, 2001]. The top of the low velocity volume is determined to lie at a depth of 6 ± 2 km from the differential delays of first arrival data [*Kleffman et al.*, 1998].

Tomography solutions that use all the SIGHT explosion data and natural earthquakes also show that rocks within the Alpine fault zone have unusually low seismic P-wave velocities. Southwest of Haast, a vertical seismic low-velocity zone is imaged to at least 15 km depth [*Eberhart-Phillips and Bannister*, 2002]. In central South Island, a localised 4-10% velocity reduction is consistent with a moderately southeast-dipping fault zone over a fault length of 50-100 km that penetrates to a depth of 20-30 km [*Stern et al.*, 2001; *Eberhart-Phillips and Bannister*, 2002; *Scherwath et al.*, 2003; *Van Avendonk et al.*, 2004].

Alpine fault rocks may have low seismic velocity because of gouge, high crack density and high pore fluid pressure [*Eberhart-Phillips*, 1995]. Temperature and strain anomalies may be contributing factors, particularly in the fully ductile zone; laboratory measurements of metagreywacke show that the inferred temperature increase can cause 1-2 % velocity reduction at 15-30 km depths [*Christensen and Mooney*, 1995]. Active straining of rock produces small decreases in velocity, as observed in laboratory studies of dynamic moduli [*Winkler and Murphy*, 1995]. The combination of very low seismic velocity (6-10% reduction) and high electrical conductivity (30-300 ohm-m) at depths of 10-30 km suggests that pore fluid is both interconnected and at pressures approaching lithostatic [*Jones and Nur*, 1984; *Wannamaker et al.*, 2002]. The source of the pore fluids may be prograde metamorphism within the crustal root; large volumes of fluid may not be required because the rocks are likely to have low porosity.

HIGH HEAT FLOW AND GEOTHERMAL GRADIENT

Observational evidence

A small number of direct heat-flow measurements from drillhole data [*Allis and Shi*, 1995] indicate a rise from 60 ± 5 mW/m^2 offshore to a maximum of 190 ± 50 mW/m^2 in the area of greatest erosion rate adjacent to the Alpine fault near Franz Josef (corresponding to an estimated geothermal gradient of $60° \pm 15°$C/km). The large uncertainty in heat-flow measurements is due to the effects of steep topography and near-surface water circulation near the fault. Further south, near Haast, measured heat-flow near the Alpine fault is 90 ± 25 mW/m^2, suggesting a lower geothermal gradient in regions with slower exhumation rates. West of the Alpine fault and north of Franz Josef, data from 24 drillholes allow a heat-flow estimate of 75 ± 25 mW/m^2 to be made [*Townend*, 1999].

Hot springs are abundant just east of the Alpine fault in central South Island. Although the water is thought to be predominantly meteoric, water in some of the hot springs contains a minor metamorphic component, suggesting fluids partly derived from depth [*Allis et al.*, 1979; *Koons and Craw*, 1991]. It has been suggested that elevated hydrothermal circulation near the Alpine fault may result from enhanced permeability owing to late stage brittle deformation and fracture [*Allis and Shi*, 1995].

Fluid inclusions trapped within quartz veins in high-grade schists exhumed next to the Alpine fault indicate formation at high temperature and low pressure [*Craw*, 1988; *Holm et al.*, 1989; *Craw et al.*, 1994; *Jenkin et al.*, 1994]; geothermal gradients of 70-90°C/km in the top 3-4 km of the crust are inferred for the central Southern Alps. The estimated depth range is dependent on an assumed lithostatic fluid pressure gradient; if fluid pressures were hydrostatic, the estimated temperature gradients would be lower (ca. 25-35°C/km). Fluid inclusions may record transient, high-stress, high fluid pressure conditions associated with earthquakes, rather than typical conditions [*Allis and Shi*, 1995].

Thermochronological data indicate rapid cooling close to the Alpine fault. Fast erosion and exhumation have produced a pattern of decreasing metamorphic grade and increasing thermochronological age with increasing distance from the fault, consistent with the effects from rapid uplift and exhumation since ca. 5 Ma in central South Island [*Adams and Gabites*, 1985; *Tippett and Kamp*, 1993; *Batt and Braun*, 1999; *Batt et al.*, 2004; *Little et al.*, 2005].

Conclusions from thermo-mechanical models

Thermal and thermo-mechanical models show that rapid exhumation along the Alpine fault inevitably perturbs isotherms to shallower depths, increasing the geothermal gradient in the vicinity of the fault and causing elevated heat-flow above it [*Allis et al.*, 1979; *Koons*, 1987; *Allis and Shi*, 1995; *Beaumont et al.*, 1996; *Batt and Braun*, 1999; *Gerbault et al.*, 2003]. An additional heat source (neglected in most models) is frictional shear heating [*Scholz et al.*, 1979], although the effect will only be significant if the fault has considerable shear strength. Assuming hydrostatic fluid pressure and a reasonable strength profile along the fault with depth, it has been shown that models without frictional shear heating fit heat-flow and thermochronological data at least as well as, or better than, models that include shear heating [*Shi et al.*, 1996].

Significant variations occur between different published thermo-mechanical models of the Southern Alps: some show a maximum upward deflection of 100-300°C isotherms east of the surface trace of the Alpine fault, matched by a downward perturbation of higher temperatures to the west and at greater depths as material is deflected downwards into a thickening crustal root [*Allis and Shi*, 1995; *Gerbault et al.*, 2003]; whereas others place the elevated 400°C isotherm directly above the Alpine fault at extremely shallow (< 5 km deep) levels [*Koons*, 1987; *Batt and Braun*, 1999]. While differences exist, all the models predict elevated heat-flow above the Alpine fault is a consequence of rapid exhumation of lower crustal material. It follows that the highest exhumation rates, which are found near Franz Josef [*Tippett and Kamp*, 1993; *Batt et al.*, 2004; *Little et al.*, 2005], have led to a greater perturbation of isotherms and an increase in heat-flow in that region. Mechanical models of the Alpine fault demonstrate how elevated heat-flow and temperatures near the fault can cause a shallowing of the transition between brittle and ductile behaviour, so that the "locking depth" (i.e., the depth to which the fault remains essentially undeforming between earthquakes) is reduced [*Ellis and Stöckhert*, 2004b; *Ellis et al.*, 2006]. Mechanical models and geochemical observations also indicate that coupling between deformation and fluid

flow may play an important role in allowing meteoric fluids to penetrate to depths where ductile rock deformation is occurring [*Upton et al.*, 1995].

ALPINE FAULT LOCKING INFERRED FROM GEODETIC DATA

Beavan et al. [1999] interpreted the velocity field from GPS surveys between 1994 and 1998 in a ~100-km wide swath across the South Island through the central Southern Alps. They modeled the data using a two-fault model, one being the Alpine fault and the other dipping in the opposite direction with a deeper locking depth; this eastern fault was required to fit distributed surface deformation within the Alps and in reality is likely to be accommodated by numerous faults. Modeled Alpine fault strike-slip rates were lower than those inferred geologically, dip-slip rates were higher, and a shallow model locking depth of 5-8 km was obtained [*Beavan et al.*, 1999].

Pearson et al. [2000] modeled surface velocities from two GPS surveys in 1995 and 1998 that crossed the Southern Alps in a ~20-km wide transect near Haast, just north of where the fault is believed to be vertical and dip-slip motion is small. Modeling was done by grid search on slip rate and locking depth, with other parameters held fixed: first for a one-fault model, and then for a two-fault model similar to that used by *Beavan et al.* [1999]. The one-fault model gave a locking depth of ~20 km, which is greater than the 12 km maximum depth of recorded earthquakes. The two-fault model was best fit with a 10±2 km Alpine fault locking depth, a strike slip rate slightly slower than geological estimates and a dip slip rate rather faster [*Pearson et al.*, 2000].

The previously described studies suffer from interpreting the velocity or strain-rate field projected onto a profile. In contrast, *Wallace et al.* [submitted] interpreted the velocity field of the South Island in a single model that solves for long-term rotations of crustal blocks, coupling distribution (the proportion of slip released episodically) along faults forming the block boundaries, and uniform strain fields within the blocks [*McCaffrey*, 2002]. For the ~200 km length of the Alpine fault in central South Island, they assumed a 45° dipping Alpine fault as one block boundary, and a distributed network of faults following the eastern foothills of the Alps as another. Geological slip rate and Australia-Pacific relative plate motion constraints were applied and both along-strike and down-dip variations in coupling were solved for, assuming the coupling coefficient decreases monotonically with depth. Wallace et al. [*submitted*] were able to fit the GPS velocities with two possible models. (1) A model with a coupling coefficient averaging 70-85% down to 18 km depth, with slightly lower coupling values on the central Alpine fault. In this model, 70% locking to 18 km depth gives surface deformation roughly equivalent to 100% locking to about 15 km depth, which is still deeper than the maximum depth of small and moderate earthquakes. Alpine fault strike-slip rates for this model were at the high end of geological estimates (31 mm/yr) and dip-slip rates were similar to geological estimates [*Wallace et al.*, submitted]. (2) A model fitting the GPS velocities with an Alpine Fault strike-slip rate of 27 mm/yr (closer to the mid-point of geological estimates), and up to 5 mm/yr of distributed dextral deformation within the Southern Alps (< 50 km to the east of the Alpine Fault). In this model the coupling coefficients on the Alpine fault were smaller than in the first model, particularly in the central 80 km (reduced to 50% coupling) [*Wallace et al.*, submitted]. However, both cases require substantial interseismic coupling on the Alpine fault to match GPS observations.

DISCUSSION: ALPINE FAULT RUPTURE MECHANISMS

A long-term slip rate of 2-3 cm/yr on a discrete Alpine fault plane in the shallow surface (top 1 km) is demonstrated by geological observations [*Berryman et al.*, 1992;

Yetton et al., 1998; *Norris and Cooper*, 2001], but undeformed river terraces and man-made structures, and small aperture resurveyed networks convincingly show that no slip has occurred on the Alpine fault plane during the last 40-100 yr. Therefore, the Alpine fault must move episodically.

Globally, episodic movement on faults in the upper crust most commonly occurs during earthquakes [*Scholz*, 2002]. Seismological and geodetic observations suggest that the Alpine fault in central South Island is locked above a depth of 7-12 km and may fail during earthquakes [*Eberhart-Phillips*, 1995; *Beavan et al.*, 1999; *Leitner et al.*, 2001]. Direct evidence for previous Alpine fault earthquakes comes from the occurrence of pseudotachylyte within fault rocks and stratigraphic evidence for episodic scarp formation accompanied by liquefaction of adjacent sandy horizons.

However, in the past decade there has been increasing awareness that earthquakes only account for a fraction of plate boundary displacements, as predicted by models of present day plate velocities [*DeMets*, 1997]. The advent of continuous, coeval and collocated GPS and seismic measurements has revealed a suite of processes that may account, at least in part, for this slip deficit. These processes include slow-rupture earthquakes, silent earthquakes, aseismic creep and afterslip. For example, in both Japan [*Heki et al.*, 1997] and Kamchatka [*Burgmann et al.*, 2001], seismic events of around M_w=7.6 were followed by afterslip for a period of ca. 12 months after the main event. In both cases, the afterslip events had a seismic moment greater than or equal to the main seismic event. So called "tsunami earthquakes" are also types of slow earthquake in the sense that the magnitudes of such events appear deceptively small when measured at the standard 20 s period, but are much larger when estimated from long period (~250 s) surface waves [*Kanamori and Kikuchi*, 1993]. Slow earthquakes and other forms of aseismic fault slip are generally, but not solely, linked to evidence for high fluid pressures [*Kanamori and Kikuchi*, 1993; *Kennedy et al.*, 1997; *Dragert et al.*, 2001; *Obara*, 2002; *Douglas et al.*, 2005].

For models of rate and state dependent friction, high fluid pressures and a high geothermal gradient reduce the effective normal stress on the fault and suppress velocity weakening of the fault, and hence stable sliding, rather than stick-slip (earthquake) behaviour is promoted [*Scholz*, 1998; *Scholz*, 2002]. Both these characteristics are present in central South Island, so the suggestion that some earthquakes in the central region involve a transitional steady/unsteady style of frictional failure (i.e., slow earthquakes) remains plausible [*Stern et al.*, 2001]. However, petrological and structural evidence suggest that the 2-3 km thick Alpine fault mylonite zone is relatively dry above 5-10 km depth [*Vry et al.*, 2001]. Moreover, there is evidence from the geology and geometry of the electrical conductivity anomaly that water from the fault zone is released vertically ~8 km from the surface trace of the Alpine fault. Isotopic measurements show that a meteoric component is present in fluids that exist within the Alpine fault zone at depths of ~6-8 km, requiring some circulation of fluids from the surface to that depth [*Upton et al.*, 1995]. Hence, we suggest that, although the deepest parts of the Alpine fault may have near-lithostatic fluid pressures, the Alpine fault zone is not overpressured at depths <8 km, and will behave in a similar fashion to other shallow crustal faults and is likely to fail during earthquakes.

It may also be that the dynamics of the earthquake cycle are actually essential to produce the observed pattern of strain localisation in the mid and lower crust. Model experiments in which brittle slip on the Alpine fault occurs episodically show that an upper crustal earthquake may cause stress concentration in the mid-crust, resulting in a long-term strain pattern that is similar in geometry to the seismic velocity and electrical conductivity anomalies observed in central South Island [*Ellis and Stöckhert*, 2004a].

We suggest that earthquakes are likely to occur on the Alpine fault in central South Island, but important questions remain: what is the maximum earthquake magnitude, and what proportion of Alpine fault displacement is accommodated aseismically or in small or moderate magnitude earthquakes? Geological arguments of fault continuity, single event displacement, and coincidence of forest damage and landslides at widely-spaced localities near the Alpine fault have led numerous authors to conclude that the Alpine fault may fail in a great earthquake of M_w ~8.0 [*Adams*, 1980; *Berryman et al.*, 1992; *Sutherland and Norris*, 1995; *Bull*, 1996; *Berryman et al.*, 1998; *Wells et al.*, 1998; *Yetton*, 1998; *Wells et al.*, 1999; *Leitner et al.*, 2001]. However, great strike-slip earthquakes have rupture dimensions of several hundred km [*Wells and Coppersmith*, 1994; *Hanks and Bakun*, 2002]. If local regions of the Alpine fault in central South Island have had stress relieved at all but shallow depths because the fault has already slipped in that region, do these regions inhibit earthquake ruptures from propagating and hence limit the maximum earthquake magnitude that is possible? We constructed a simplified dynamic rupture model to test this hypothesis.

ALPINE FAULT DYNAMIC RUPTURE MODEL

The model fault is 100 km long and 12 km deep and has a rectangular patch at depth with zero initial shear stress (Fig. 3). The patch simulates a region that has slipped due to elevated temperature and fluid pressure. Based on the observed pattern of seismicity, a 25 km long patch with an upper limit at 6 km depth was considered realistic, but other lengths and upper limits were also tested.

We use a 3-D finite-difference computer program to simulate dynamic rupture of a strike-slip fault [*Harris and Day*, 1999]. The earthquake is artificially nucleated over a small area and then allowed to spontaneously propagate. The rupture velocity and the temporal and spatial patterns of rupture are not prescribed, but result from stress conditions on each sub-segment at each point in time. A slip-weakening fracture criterion is incorporated, so that the shear strength of the fault linearly decreases from a high static value to a low dynamic value after slipping a critical distance, d_0. Thus, it is much easier for an earthquake to continue to propagate once it is large enough and is only working against dynamic friction.

Taking parameter values calibrated to realistic models of the 1999 M_w=7.4 Izmit, Turkey, earthquake [*Harris et al.*, 2002], we used critical slip (d_0) of 20 cm, static friction (μ_s) of 0.677, and dynamic friction (μ_d) of 0.525. Most model runs were for high-stress, below-failure conditions on the brittle fault segments with average initial stress (τ_0) of 70 MPa, and initial normal stress (σ_n) of 120 MPa. The fault segments are defined with zero cohesion so their static and dynamic yield strengths are 81 MPa and 63 MPa, respectively. The rest of the 3-D volume is assigned very high cohesion. To represent the decrease in stress toward the free surface, we include a linear taper over the upper 3 km for both τ_0 and σ_n. Actual shear stress is unlikely to be uniform, so a stochastic model is used to define τ_0 on the brittle fault (Fig 3). This is a 2-D self-similar random function with 2 km shortest wavelength, and variations up to ±6 MPa, giving the fault varied stress drop ranging from 1 to 13 MPa. The nucleation point is put near the end of the fault and in a region of the stochastic model that has a reasonably high τ_0.

The results of the numerical models are summarized in Fig 3, which shows the range of patch lengths and upper limits that were investigated. For a zero shear stress patch with length 25 km and an upper limit of 6 km, the rupture is able to continue to the far end of the fault, and propagates within the patch. With the upper limit of the patch raised to 3 km, the rupture still continues along the entire fault. Only when the upper limit is at <2 km does the rupture get suppressed and only part of the region above the

patch is ruptured. For shorter patch lengths, shallower upper limits of the patch are required to stop the rupture. For a 7 km long patch, a >1 km depth brittle section is required to allow rupture to continue to the end of the fault. The rupture can jump over a 1 km long patch that reaches the surface, but rupture propagation is stopped by a 2 km long patch that reaches the surface.

The choice of nucleation point influences whether the earthquake turns into a full-length rupture. All models in Fig. 3 have a distant nucleation point, but we also ran models with other nucleation points. When the rupture was nucleated at a point on the fault that was close to the patch, the rupture did not make it fully across a patch of width 25 km and upper limit 6 km. If the rupture was nucleated above the ductile patch, it was not able to rupture into the section with normal brittle behaviour to a depth of 12 km. Slip velocity and stress concentration at the leading edge of the rupture scales with fault depth, and thus it is more difficult for an initial 6 km depth rupture to grow into a 12 km depth rupture, than vice versa [*Harris and Day*, 1993].

The length of rupture along a fault with a varied depth of rupture is not dependent on whether it is high-stress or low-stress, but the low-stress case displayed some overshoot. We tested a series of fault models with low-stress conditions [*Harris et al.*, 2002]. The rupture patterns of the brittle fault were virtually the same as under high-stress conditions. However, there was an intriguing difference within the patch. For low-stress initial conditions, the rupture penetrates into the patch, even though no slip is required there. If such overshoot regularly occurs along an individual fault segment, it could have long-term effects, such as further localizing faulting on that segment.

Although the model is highly simplified, it clearly suggests that stress relief by creep or unstable sliding on a patch of the deeper part of the fault (>6 km depth) is insufficient to stop a fully developed earthquake rupture from propagating along the shallow part of the locked fault. However, a patch that has crept at depth may inhibit a large rupture from nucleating above it.

DISCUSSION: ALPINE FAULT RUPTURE SCENARIOS

We have established a strong case that the shallow part (<6-12 km depth) of the Alpine fault in central South Island is locked and capable of failing in an earthquake, but the maximum magnitude of any such earthquake depends upon how far that rupture propagates. Our model results indicate that patches of low shear stress, with dimensions that we consider to be realistic for a slow earthquake, are unlikely to stop the dynamic rupture of a large or great earthquake along the Alpine fault in central South Island; the precursory slip would have to reach depths of <1-4 km over a significant length of fault (>10-30 km) to inhibit a rupture.

Geometric irregularities of the fault surface are another factor that can influence rupture. Rupture simulations show that a strike-slip rupture can jump across gaps of <5 km between fault segments [*Harris and Day*, 1999]: moderate-sized earthquakes cascade into larger earthquakes e.g. the 1992 M_w=7.3 Landers, California, earthquake ruptured four fault segments. The 1999 M_w=7.4 Izmit, Turkey, earthquake jumped several step-overs and propagated around a bend, but did not jump step-overs greater than 5 km [*Harris et al.*, 2002]. The 1855 M_w=8.2 Wairarapa, New Zealand, earthquake ruptured across step-overs up to 6 km wide [*Schermer et al.*, 2004]. Ruptures may also change direction and transfer slip to adjacent faults with different strike: for example, the 2002 M_w=7.9 Denali earthquake ruptured three segments, each of which differs in strike by 20-30° [*Eberhart-Phillips et al.*, 2003]. The differing-rake segments of the Alpine fault have no gap at the surface and this type of 'serial partitioning' of the surface trace is probably a response to erosional processes in operation at the range front

[*Norris and Cooper*, 1997]. Thus, we suggest that the minor (<5 km) fault step-overs and changes in Alpine fault dip at the surface are not sufficient by themselves to inhibit a fully developed rupture that penetrates through the entire depth of the locked zone.

A number of scenarios remain for the possible rupture dimension of earthquakes on the central part of the Alpine fault (Fig. 1). Theoretical considerations indicate that large or great earthquakes could occur, but cannot prove that they do. Does a combination of low shear stress and rough fault plane geometry inhibit ruptures in central South Island? Is the Alpine-Hope fault intersection a natural barrier to rupture? Could a rupture propagate between the Alpine and Hope faults? What is the significance of changes in hanging wall uplift rate, fault dip, and local segmentation style near Haast, and is this related to complexity at depth that could inhibit a rupture? Where might the southern limit of a fault rupture on the central Alpine fault be located: Haast River, Cascade River, Caswell Sound, Puysegur subduction thrust, or somewhere between? Where might the northern limit be?

The history of past earthquakes (Table 1; Fig. 1) provides some guide as to what is possible in future. Radiocarbon data from trenches in the Haast-Okuru region indicate two coseismic displacement events of 8-9 m after c. 1160 AD, and three since c. 700-800 AD [*Berryman et al.*, 1998]. Estimated ages of forest disturbance at 1650-1725 AD [*Cooper and Norris*, 1990] and 1700-1730 AD [*Wells et al.*, 1998] near to the Alpine fault are correlated with terrace abandonment at Karangarua River at 1710-1720 AD and a major tree growth suppression event at 1717 AD [*Wells et al.*, 1999], which is inferred to be the year of the last Alpine fault earthquake. Evidence for the 1717 AD event spans a distance of c. 400 km from Te Anau to Taramakau River and is associated with 8-9 m offsets at localities between Milford Sound and Haast. A trench at Crane Creek, a tributary of Ahaura River, demonstrates that surface rupture associated with this event died out 25-35 km northeast of the Taramakau River and the intersection with the Hope fault [*Yetton et al.*, 1998]. It is not known if the western segment of the Hope fault was also ruptured during this event [*Langridge and Berryman*, 2005].

At Karangarua River (Fig. 1) there is evidence for an uplift and terrace abandonment event at 1600-1620 AD [*Yetton et al.*, 1998] and this corresponds to the time of a significant forest disturbance at 1610-1640 in the northern region [*Wells et al.*, 1998] and near Franz Josef [*Cullen et al.*, 2003], and of tree-ring suppression at c. 1620 AD at Waitaha River [*Wright*, 1998]. The event is not recorded as far south as Haast [*Berryman et al.*, 1998; *Yetton et al.*, 1998], but is recorded north of the Hope fault intersection at Ahaura River [*Yetton et al.*, 1998] and 35 km southwest of Lake Rotoiti [*Yetton*, 2002].

The Karangarua River terrace abandonment event at 1405-1445 AD [*Yetton et al.*, 1998], the significant forest disturbance event at 1410-1440 AD [*Wells et al.*, 1998], and a radiocarbon date of 1420-1450 AD from a large rock avalanche near Lake Kaniere [*Yetton et al.*, 1998] all suggest that this was the time of a significant earthquake (Fig. 1). The penultimate event identified from trenching in the Haast-Okuru area is constrained by radiocarbon evidence to have an age in the range 1160-1410 AD [*Berryman et al.*, 1998], though some of the dated material was clearly recycled from older sediment - leaving the likely possibility that the event is younger than stated. We propose two possibilities: either a single event at c. 1430 AD ruptured the Alpine fault from south of Turnbull River to north of Ahaura River; or the rupture extent was only north of Haast, requiring an earlier rupture during the interval 1160-1410 AD to be the penultimate event in the Haast-Milford region. We favour the former scenario, because there is clear sedimentological evidence within the trench for reworking of the youngest soil into the the fault scarp colluvial wedge [*Berryman et al.*, 1998], and suggest that an

earthquake in c. 1430 AD ruptured the Alpine fault from north of the Hope fault intersection to at least as far south as Milford Sound.

DISCUSSION: MAXIMUM EARTHQUAKE MAGNITUDE

Although paleoseismic data are relatively sparse and imprecise (Table 1), sufficient exist to evaluate the probable extent of the last three Alpine fault ruptures: the 1717 AD event is inferred to have ruptured a 300-500 km length of fault; the 1620 AD event ruptured 200-300 km; and the 1430 AD event ruptured 350-600 km (Table 1; Fig. 1). If it is assumed that these events were single ruptures with an average down-dip rupture dimension of 12 km, then their respective magnitudes (M_w), as inferred from comparisons with similar global examples [*Hanks and Bakun*, 2002; *Lin et al.*, 2002; *Eberhart-Phillips et al.*, 2003], were 7.9 ± 0.3, 7.6 ± 0.3, and 7.9 ± 0.4.

Could the assumption that each paleoseismically recorded event corresponds to a single earthquake be wrong? The paleoseismic record allows us to determine: synchroneity to a precision of c. 1-10 years for the last event (1717 AD) and c. 10-50 years for the two previous events (c. 1620 and 1430 AD); and that 8-9 m of slip occurred in the 1717 and 1430 AD events in the Milford-Haast region (Table 1; Fig. 1). We accept that several earthquakes and some afterslip during a single interval of several years could combine to produce a pattern of fault displacement that is consistent with the paleoseismic evidence. If sections of Alpine fault of length 80-100 km ruptured during a sequence, then each event is inferred to have magnitude $M_w = 7.2 \pm 0.3$ [*Wells and Coppersmith*, 1994]. While earthquake clustering in space and time can occur through various stress transfer mechanisms [*Freed*, 2005], the relative scarcity of global examples where a single continuous fault has ruptured in this manner, and the results of our dynamic rupture modeling, lead us to suggest that this is an unlikely scenario for the Alpine fault.

CONCLUSIONS

Geological observations require that episodic slip on the Alpine fault averages to a long-term displacement rate of 2-3 cm/yr. Patterns of natural seismicity and geodetic strain suggest that the Alpine fault in central South Island (between Haast and Taramakau River) is currently locked above a depth of 6-12 km and will probably fail in an earthquake.

In addition to earthquakes, aseismic slip at shallow crustal depths (6-12 km) may play a role in accommodating long-term fault displacement; this conclusion is made on the basis of high pore fluid pressures inferred from the very low seismic P-wave velocity and high electrical conductivity of the Alpine fault zone, and by comparison with other faults with high inferred fluid pressures and a record of aseismic slip.

Our modeling suggests that an episode of aseismic slip at depth may inhibit the nucleation of a large earthquake in the region above it, but is unlikely to inhibit the propagation of a fully developed rupture during a large or great earthquake. We did not investigate the stress loading of adjacent parts of the fault plane during a possible slow-slip event, and acknowledge that our model is highly simplified. However, our conclusion is supported by a comparison with subduction zones, which are where most slow-slip earthquakes are documented, where high pore fluid pressures are inferred, but also where most great earthquakes occur.

A range of maximum earthquake magnitudes may be possible on the Alpine fault, depending on what length of fault ruptures. Based upon physical models that are calibrated using data from earthquakes elsewhere, we infer that: the observed Alpine fault geometry (Fig. 1) is sufficiently smooth to allow ruptures to propagate; and low-

stress patches on the fault are unlikely to inhibit a fully developed rupture from propagating. However, the combination of along-strike changes in Alpine fault geometry, thermal structure, fluid pressure, interactions with other faults, the possibility of episodic strain release at depth, and our inadequate knowledge of the spatially variable material properties and stress field means that our physical models are substantially over-simplified. It is, therefore, essential that any predictive model is consistent with past Alpine fault behaviour.

Past earthquakes on the central Alpine fault are inferred to have ruptured at least as far south as Fiordland (ca. 1717 AD; ca. 1430 AD) or to have been limited to the region north of Haast (ca. 1620 AD), and to have ruptured north to the Taramakau River (ca. 1717 AD) or to at least as far north as Ahaura River (ca. 1620 AD; ca. 1430 AD). Each of the three events documented is inferred to have different rupture dimensions (Table 1; Fig. 1) and magnitudes: the 1620 AD event is inferred to have the most limited rupture extent (200-300 km); the 1430 AD event is inferred to have the largest rupture extent (350-600 km); and the 1717 AD event is intermediate (300-500 km), though it is not known if the western segment of the Hope fault was also ruptured during this event. Based upon the assumption that the paleoseismic events occurred in single earthquakes, the last three earthquakes most likely had magnitudes (M_w) in the range 7.6-7.9. We cannot rule out the possibility that some paleoseismically recorded events may be composed of a sequence of triggered earthquakes with smaller magnitude, but consider this scenario unlikely.

We conclude that large earthquakes ($M_w > 7$) on the Alpine fault will almost certainly occur in future. Great earthquakes ($M_w \geq 8$) with rupture dimensions of several hundred km are consistent with and provide a reasonable explanation for paleoseismic data, and hence remain a realistic future scenario. Better delineation of fault properties and structure at depth is required to allow more realistic models of Alpine fault earthquake rupture to be developed. Additional paleoseismic observations that improve the spatial extent of timing and displacement data, and sample a greater period of time (more past events) are required to test whether predictive models can accurately hindcast earthquakes.

Finally, we hypothesise that slow-slip events could occur at moderate depths (5-20 km) on the Alpine fault, and that a relationship may exist between the timing of such events and the nucleation of earthquakes. We suggest that continuous recording of GPS and seismicity data, and possibly some type of repeated stress measurement, around regions of high inferred fluid pressure (Fig. 1) is required to test this hypothesis, record what actually happens during the next significant Alpine fault earthquake, and ultimately to provide a basis for time-varying seismic hazard estimates.

TABLE

Table 1. Summary of Alpine fault paleoseismic data (from north to south)

Region	Paleoseismic evidence
Wairau fault	No rupture during last c. 2000 yr [*Zachariasen et al.*, 2006].
Lake Rotoiti to Springs Junction	Last slip event of 1-2 m at 1455-1700 AD; probably c. 1620 AD, based on forest disturbance [*Yetton*, 2002]. No fault creep at roads or at the Evison monitoring wall constructed in 1964 near Springs Junction [*Beanland*, 1987].
Ahaura River	Trenching gives last slip event at 1480-1645 AD; probably c. 1620 AD, based on forest disturbance [*Yetton*, 1998]. No fault creep at road.
Taramakau River	No fault creep at road.
Western Hope Fault	Single event dextral displacements of 3-4 m at recurrence interval of 310-490 yr, but timing of most recent surface ruptures is unknown [*Langridge and Berryman*, 2005].
Near Lake Kaniere	Trenching, forest disturbance, and tree ring data suggest earthquake events at 1717 and c. 1620 AD [*Yetton*, 1998; *Wells et al.*, 1999].
Waitaha River	Tree ring and forest disturbance ages indicate earthquakes at 1717 AD and c. 1620 AD [*Wright*, 1998; *Wells et al.*, 1999].
Near Franz Josef	Significant forest disturbance at 1717, c. 1620 and c. 1430-1450 AD [*Wells et al.*, 1999], and forest establishment on floodplains just after c. 1720 AD and c. 1620 AD [*Cullen et al.*, 2003]. No fault creep at road or within Franz Josef village.
Karangarua River	Significant forest disturbance at c. 1710–20, 1610–20 and 1460 AD [*Wells et al.*, 2001] coincide with uplift and terrace abandonment events [*Adams*, 1980; *Yetton*, 1998].
Haast, Turnbull, and Okuru rivers	Dextral displacements of 8-9 m during last two events. Trenching indicates three events since 700-800 AD, with the penultimate event (see main text) at c. 1430 AD [*Berryman et al.*, 1998]. Tree-ring suppression in a tree on the fault trace suggests the last event was at c. 1720 AD [*Berryman et al.*, 1998]. No fault creep at road.
Hokuri Creek	Dextral displacements of 8-9 m during last two events, with last event at 1600-1800 AD [*Sutherland and Norris*, 1995].
Milford Sound	Tree damage near fault scarp indicates last displacement at 1650-1725 AD [*Cooper and Norris*, 1990] and regional tree-ring suppression at c. 1717 AD [*Wells et al.*, 1999].

FIGURES
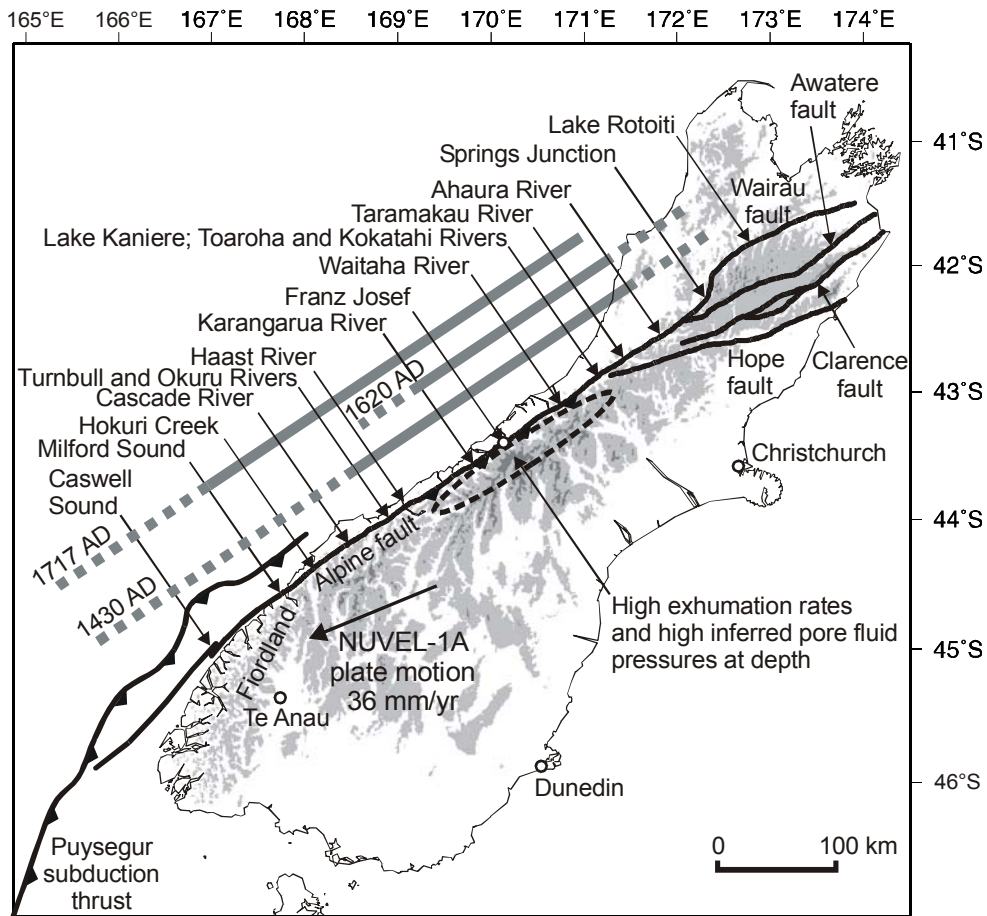
Figure 1. Location of the Alpine fault and places named in the main text. Topography >800 m is shown with a light shade and >1800 m with a dark shade. Bold grey lines indicate inferred extent of past Alpine fault ruptures. Bold arrow shows NUVEL-1A Pacific-Australia plate motion [*DeMets et al.*, 1994].
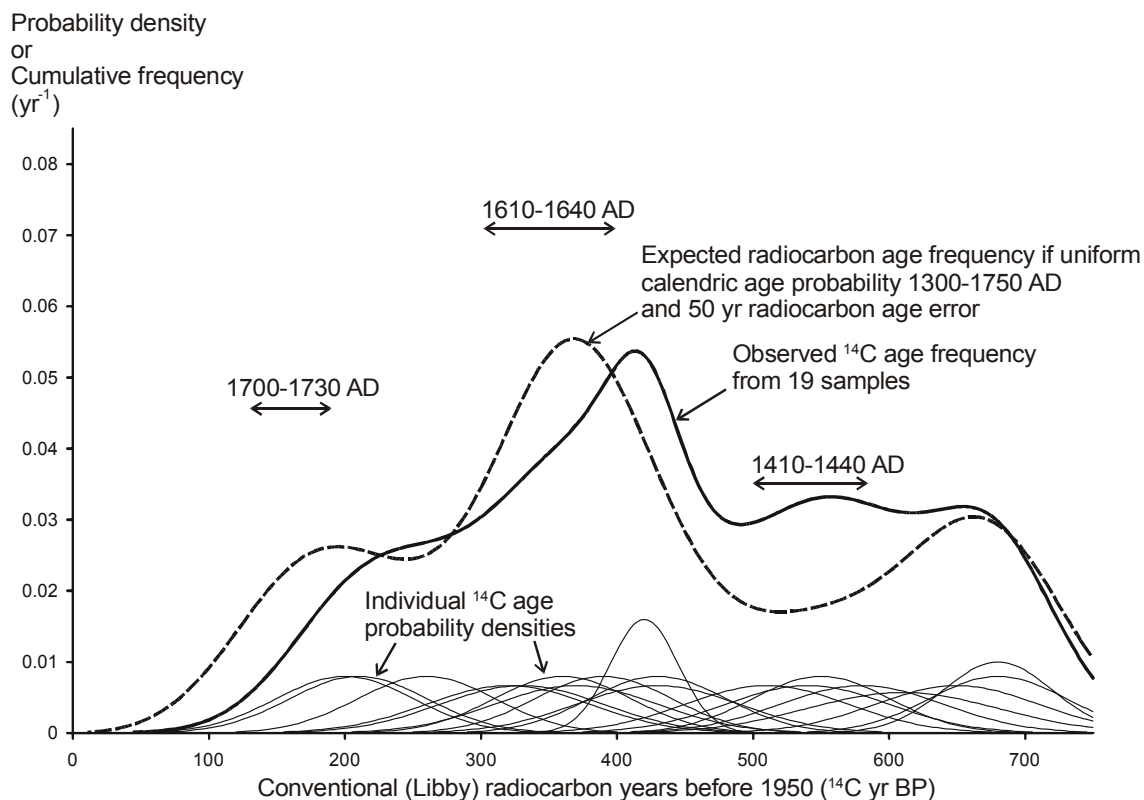
Figure 2. Radiocarbon ages from aggradation and mass-movement deposits inferred to be younger than 1250 AD [*Yetton*, 1998; *Yetton et al.*, 1998]. Thin lines show probability densities for individual samples. Bold line shows cumulative frequency, derived by summing the individual probability densities. The dashed line is the cumulative frequency expected from the SHCAL04 dataset [*McCormac et al.*, 2004], assuming the null hypothesis that the true calendric age of wood samples is equally likely during the interval 1300-1750 AD. The expected radiocarbon age ranges of inferred forest disturbance events at 1700-1730 AD, 1610-1640 AD, and 1410-1440 AD are also indicated [*Wells et al.*, 1998].
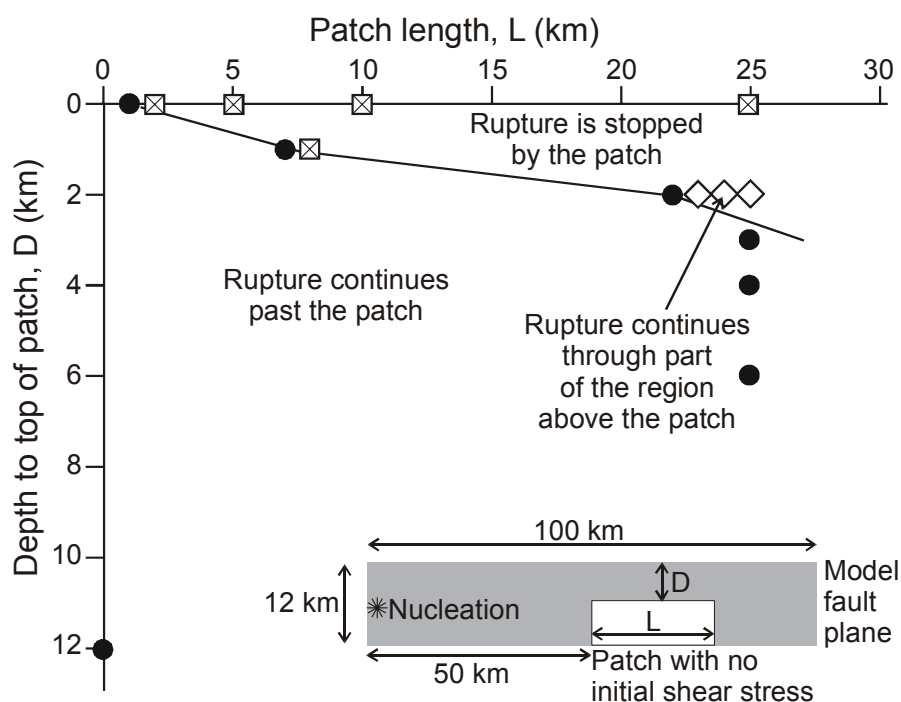
Figure 3. Rupture propagation model results showing the range of zero shear stress patch lengths, L, and shallow depth limits, D, that inhibit a dynamic rupture above the patch. The patch simulates a region of the fault that has slipped and had all shear stress relieved. Model runs are shown in which the rupture: successfully propagated past the patch (filled circles); propagated through part of the region above the patch (diamonds); and was completely stopped by the patch (checked squares).

REFERENCES

Adams, C.J., and J.E. Gabites, Age of metamorphism and uplift in the Haast Schist Group at Haast Pass, Lake Wanaka and Lake Hawea, South Island, New Zealand, *New Zealand Journal of Geology and Geophysics*, *28* (1), 85-96, 1985.

Adams, J., Paleoseismicity of the Alpine Fault seismic gap, *Geology*, *8*, 72-76, 1980.

Allis, R.G., R.W. Henley, and A.F. Carman, The thermal regime beneath the Southern Alps, *Bulletin of the Royal Society of New Zealand* (18), 79-85, 1979.

Allis, R.G., and Y. Shi, New insights to temperature and pressure beneath the central Southern Alps, New Zealand, *New Zealand Journal of Geology and Geophysics*, *38* (4), 585-592, 1995.

Barnes, P.M., R. Sutherland, B. Davy, and J. Delteil, Rapid creation and destruction of sedimentary basins on mature strike-slip faults: an example from the offshore Alpine Fault, New Zealand, *Journal of Structural Geology*, *23*, 1727-1739, 2001.

Barnes, P.M., R. Sutherland, and J. Delteil, Strike-slip structure and sedimentary basins of the southern Alpine Fault, Fiordland, New Zealand, *Geological Society of America Bulletin*, *117*, 411-435, 2005.

Batt, G.E., S.L. Baldwin, M.A. Cottam, P.G. Fitzgerald, M.T. Brandon, and T.L. Spell, Cenozoic plate boundary evolution in the South Island of New Zealand; new thermochronological constraints, *Tectonics*, *23* (4), 17, 2004.

Batt, G.E., and J. Braun, The tectonic evolution of the Southern Alps, New Zealand: insights from fully thermally coupled dynamical modelling, *Geophysical Journal International*, *136*, 403-420, 1999.

Beanland, S., Field guide to sites of active earth deformation, South Island, New Zealand, *New Zealand Geological Survey Record*, *19*, 1-104, 1987.

Beaumont, C., P.J.J. Kamp, J. Hamilton, and P. Fullsack, The continental collision zone, South Island, New Zealand: comparison of geodynamical models and observations, *Journal of geophysical research*, *101* (B2), 3333-3359, 1996.

Beavan, J., M. Moore, C. Pearson, M. Henderson, B. Parsons, S. Bourne, P. England, R.I. Walcott, G. Blick, D. Darby, and K. Hodgkinson, Crustal deformation during 1994-98 due to oblique continental collision in the central Southern Alps, New Zealand, and implications for seismic potential of the Alpine fault, *Journal of Geophysical Research*, *104* (B11), 25233-25255, 1999.

Berryman, K., A.F. Cooper, R.J. Norris, R. Sutherland, and P. Villamor, Paleoseismic investigation of the Alpine Fault at Haast and Okuru, *Geological Society of New Zealand miscellaneous publication*, *101A*, 44, 1998.

Berryman, K.R., S. Beanland, A.F. Cooper, H.N. Cutten, R.J. Norris, and P.R. Wood, The Alpine fault, New Zealand: variation in Quaternary structural style and geomorphic expression, *Annales Tectonicae*, *6*, 126-163, 1992.

Bossiere, G., Petrology of pseudotachylytes from the Alpine Fault of New Zealand, *Tectonophysics*, *196*, 173-193, 1991.

Bull, W.B., Prehistorical earthquakes on the Alpine fault, New Zealand, *Journal of geophysical research*, *101*, 6037-6050, 1996.

Burgmann, R., M.G. Kogan, V.E. Levin, C.H. Scholz, R.W. King, and G.M. Steblov, Rapid aseismic moment release following the 5 December, 1997 Kronotsky, Kamchatka, earthquake, *Geophysical Research Letters*, *28* (7), 1331-1334, 2001.

Christensen, N.I., and W.D. Mooney, Seismic velocity structure and composition of the continental crust; a global view, *Journal of Geophysical Research, B, Solid Earth and Planets*, *100* (6), 9761-9788, 1995.

Cooper, A.F., and R.J. Norris, Estimates for the timing of the last coseismic displacement on the Alpine Fault, northern Fiordland, New Zealand, *New Zealand Journal of Geology and Geophysics*, *33* (2), 303-307, 1990.

Cooper, A.F., and R.J. Norris, Anatomy, structural evolution, and slip rate of a plate-boundary thrust: The Alpine fault at Gaunt Creek, Westland, New Zealand, *Geological Society of America Bulletin*, *106*, 627-633, 1994.

Cooper, A.F., and R.J. Norris, Displacement on the Alpine Fault at Haast River, South Westland, New Zealand, *New Zealand Journal of Geology and Geophysics*, *38* (4), 509-514, 1995.

Craw, D., Shallow-level metamorphic fluids in a high uplift rate metamorphic belt; Alpine Schist, New Zealand, *Journal of Metamorphic Geology*, *6* (1), 1-16, 1988.

Craw, D., M.S. Rattenbury, and R.D. Johnstone, Structures within greenschist facies Alpine Schist, central Southern Alps, New Zealand, *New Zealand Journal of Geology and Geophysics*, *37* (1), 101-111, 1994.

Cullen, L.E., R.P. Duncan, A. Wells, and G.H. Stewart, Floodplain and regional scale variation in earthquake effects on forests, Westland, New Zealand, *Journal of the Royal Society of New Zealand*, *33*, 693-701, 2003.

Davey, F.J., T. Henyey, S. Kleffmann, A. Melhuish, D. Okaya, T.A. Stern, and D.J. Woodward, Crustal reflections from the Alpine fault zone, South Island, New Zealand, *New Zealand Journal of Geology and Geophysics*, *38* (4), 601-604, 1995.

DeMets, C., Afterslip no longer an afterthought, *Nature*, *386* (6625), 549, 1997.

DeMets, C., R.G. Gordon, D.F. Argus, and S. Stein, Effect of recent revisions to the geomagnetic time scale on estimates of current plate motions, *Geophysical Research Letters*, *21*, 2191-2194, 1994.

Douglas, A., J. Beavan, L.M. Wallace, and J. Townend, Slow slip on the northern Hikurangi subduction interface, New Zealand, *Geophysical Research Letters*, *32*, L16305, doi:10.1029/2005GL023607, 2005.

Dragert, H., K. Wang, and T.S. James, A silent slip event on the deeper Cascadia subduction interface, *Science*, *292* (5521), 1525-1528, 2001.

Eberhart-Phillips, D., Examination of seismicity in the central Alpine fault region, South Island, New Zealand, *New Zealand Journal of Geology and Geophysics*, *38*, 571-578, 1995.

Eberhart-Phillips, D., and S. Bannister, Three-dimensional crustal structure in the Southern Alps region of New Zealand from inversion of local earthquake and active source data, *Journal of Geophysical Research, B, Solid Earth and Planets*, *107* (10), 20, 2002.

Eberhart-Phillips, D., P.J. Haeussler, J.T. Freymueller, A.D. Frankel, C.M. Rubin, P. Craw, N.A. Ratchkovski, G. Anderson, G.A. Carver, A.J. Crone, T.E. Dawson, H. Fletcher, R. Hansen, E.L. Harp, R.A. Harris, D.P. Hill, S. Hreinsdottir, R.W. Jibson, L.M. Jones, R. Kayen, D.K. Keefer,

C.F. Larsen, S.C. Moran, S.F. Personius, G. Plafker, B. Sherrod, K. Sieh, N. Sitar, and W.K. Wallace, The 2002 Denali Fault earthquake, Alaska; a large magnitude, slip-partitioned event, *Science*, *300* (5622), 1113-1118, 2003.

Ellis, S., J. Beavan, D. Eberhart-Phillips, and B. Stöckhert, Simplified models of the Alpine Fault seismic cycle: stress transfer in the mid-crust, *Geophysical Journal International*, *in press*, 2006.

Ellis, S., and B. Stöckhert, Elevated stresses and creep rates beneath the brittle-ductile transition caused by seismic faulting in the upper crust, *Journal of Geophysical Research*, *109* (B5), 10, 2004a.

Ellis, S., and B. Stöckhert, Imposed strain localization in the lower crust on seismic timescales, *Earth, Planets, Space*, *56*, 1103-1109, 2004b.

Evison, F.F., Seismicity of the Alpine Fault, *Royal Society of New Zealand Bulletin*, *9*, 161-165, 1971.

Freed, A.M., Earthquake triggering by static, dynamic, and postseismic stress transfer, *Annual Review of Earth and Planetary Sciences*, *33*, 335-367, 2005.

Gerbault, M., S. Henrys, and F. Davey, Numerical models of lithospheric deformation forming the Southern Alps of New Zealand, *Journal of Geophysical Research, B, Solid Earth and Planets*, *108* (7), 18, 2003.

Hanks, T.C., and W.H. Bakun, A bilinear source-scaling model for M-log A observations of continental earthquakes, *Bulletin of the Seismological Society of America*, *92*, 1841-1846, 2002.

Harris, R.A., and S.M. Day, Dynamics of fault interaction; parallel strike-slip faults, *Journal of Geophysical Research*, *98* (3), 4461-4472, 1993.

Harris, R.A., and S.M. Day, Dynamic three-dimensional simulations of earthquakes on en echelon faults, *Geophysical Research Letters*, *26* (14), 2089-2092, 1999.

Harris, R.A., J.F. Dolan, R.D. Hartleb, and S.M. Day, The 1999 Izmit, Turkey, earthquake; a 3D dynamic stress transfer model of intraearthquake triggering, *Bulletin of the Seismological Society of America*, *92* (1), 245-255, 2002.

Heki, K., S.-i. Miyazaki, and H. Tsuji, Silent fault slip following an interplate thrust earthquake at the Japan Trench, *Nature*, *386* (6625), 595-598, 1997.

Holm, D.K., R.J. Norris, and D. Craw, Brittle and ductile deformation in a zone of rapid uplift; central Southern Alps, New Zealand, *Tectonics*, *8* (2), 153-168, 1989.

Hull, A.G., and K. Berryman, Holocene tectonism in the region of the Alpine Fault at Lake McKerrow, Fiordland, New Zealand, *Royal Society of New Zealand Bulletin*, *24*, 317-331, 1986.

Jenkin, G.R.T., D. Craw, and A.E. Fallick, Stable isotopic and fluid inclusion evidence for meteoric fluid penetration into an active mountain belt; Alpine Schist, New Zealand, *Journal of Metamorphic Geology*, *12* (4), 429-444, 1994.

Jones, T., and A. Nur, Effect of temperature, pore fluids, and pressure on seismic wave velocity and attenuation in rock, *Geophysics*, *49* (5), 666, 1984.

Kanamori, H., and M. Kikuchi, The 1992 Nicaragua earthquake; a slow tsunami earthquake associated with subducted sediments, *Nature*, *361* (6414), 714-716, 1993.

Kennedy, B.M., Y.K. Kharaka, W.C. Evans, A. Ellwood, D.J. De Paolo, J.J. Thordsen, G. Ambats, and R.H. Mariner, Mantle fluids in the San Andreas fault system, California, *Science*, *278* (5341), 1278-1281, 1997.

Kleffman, S., F. Davey, A. Melhuish, D. Okaya, T. Stern, and the SIGHT team, Crustal structure in the central South Island, New Zealand, from the Lake Pukaki seismic experiment, *New Zealand Journal of Geology and Geophysics*, *41*, 39-49, 1998.

Koons, P.O., Some thermal and mechanical consequences of rapid uplift; an example from the Southern Alps, New Zealand, *Earth and Planetary Science Letters*, *86* (2), 307-319, 1987.

Koons, P.O., and D. Craw, Evolution of fluid driving forces and composition within collisional orogens, *Geophysical Research Letters*, *18* (5), 935-938, 1991.

Koons, P.O., D. Craw, S.C. Cox, P. Upton, A.S. Templeton, and C.P. Chamberlain, Fluid flow during active oblique convergence; a Southern Alps model from mechanical and geochemical observations, *Geology*, *26* (2), 159-162, 1998.

Koons, P.O., R.J. Norris, M.R. Sutherland, D. Wilson, and A.F. Cooper, Structure and activity of the Alpine Fault, north and south of Milford Sound, *Eos, Transactions, American Geophysical Union*, *75* (44, Suppl.), 669, 1994.

Langridge, R.M., and K. Berryman, Morphology and slip rate of the Hurunui section of the Hope Fault, South Island, New Zealand, *New Zealand Journal of Geology and Geophysics*, *48*, 43-57, 2005.

Leitner, B., D. Eberhart-Phillips, H. Anderson, and J.L. Nablek, A focused look at the Alpine fault, New Zealand: seismicity, focal mechanisms and stress observations, *Journal of geophysical research*, *106*, 2193-2220, 2001.

Lin, A., B. Fu, J. Guo, Q. Zeng, G. Dang, W. He, and Y. Zhao, Co-seismic strike-slip and rupture length produced by the 2001 Ms 8.1 Central Kunlun earthquake, *Science*, *296*, 2015-2017, 2002.

Little, T.A., S. Cox, J.K. Vry, and G. Batt, Variations in exhumation level and uplift rate along the oblique-slip Alpine Fault, central Southern Alps, New Zealand, *Geological Society of America Bulletin*, *117* (5-6), 707-723, 2005.

McCaffrey, R., Crustal block rotations and plate coupling, *Geodynamics Series*, *30*, 101-122, 2002.

McCormac, F.G., A.G. Hogg, P.G. Blackwell, C.E. Buck, T.F.G. Higham, and P.J. Reimer, SHCal04 Southern Hemisphere Calibration 0 - 11.0 cal kyr BP, *Radiocarbon*, *46*, 1087-1092, 2004.

Nathan, S., M.S. Rattenbury, and R.P. Suggate, *Geology of the Greymouth area, 1:250 000 geological map 12*, 58 pp., Institute of Geological and Nuclear Sciences, Lower Hutt, 2002.

Norris, R.J., and A.F. Cooper, Erosional control on the structural evolution of a transpressional thrust complex on the Alpine Fault, New Zealand, *Journal of Structural Geology*, *19* (10), 1323-1324, 1997.

Norris, R.J., and A.F. Cooper, Late Quaternary slip rates and slip partitioning on the Alpine Fault, New Zealand, *Journal of Structural Geology*, *23* (2-3), 507-520, 2001.

Norris, R.J., P.O. Koons, and A.F. Cooper, The obliquely-convergent plate boundary in the South Island of New Zealand; implications for ancient collision zones, *Journal of Structural Geology*, *12* (5-6), 715-725, 1990.

Obara, K., Nonvolcanic deep tremor associated with subduction in Southwest Japan, *Science*, *296* (5573), 1679-1681, 2002.

Okaya, D., S. Henrys, and T. Stern, Double-sided onshore-offshore seismic imaging of a plate boundary; "super-gathers" across South Island, New Zealand, *Tectonophysics*, *355* (1-4), 247-263, 2002.

Pearson, C., P. Denys, and K. Hodgkinson, Geodetic constraints on the kinematics of the Alpine Fault in the southern South Island of New Zealand, using results from the Hawea-Haast GPS transect, *Geophysical Research Letters*, *27* (9), 1319-1322, 2000.

Reed, J.J., Mylonites, cataclasites, and associated rocks along the Alpine Fault, South Island, New Zealand, *New Zealand Journal of Geology and Geophysics*, *7*, 654-684, 1964.

Schermer, E.R., R.J. Van Dissen, K. Berryman, H.M. Kelsey, and S.M. Cashman, Active faults, paleoseismology, and historical fault rupture in northern Wairarapa, North Island, New Zealand, *New Zealand Journal of Geology and Geophysics*, *47*, 101-122, 2004.

Scherwath, M., T. Stern, F. Davey, D. Okaya, W.S. Holbrook, R. Davies, and S. Kleffmann, Lithospheric structure across oblique continental collision in New Zealand from wide-angle P wave modeling, *Journal of Geophysical Research*, *108* (12), 18, 2003.

Scholz, C.H., Earthquakes and friction laws, *Nature*, *391*, 37-42, 1998.

Scholz, C.H., The mechanics of earthquakes and faulting, pp. 471, Cambridge University Press, 2002.

Scholz, C.H., J. Beavan, and T.C. Hanks, Frictional metamorphism, argon depletion and tectonic stress on the Alpine Fault, New Zealand, *Journal of geophysical research*, *84*, 6770-6782, 1979.

Shi, Y., R.G. Allis, and F. Davey, Thermal modelling of the Southern Alps, New Zealand, *Pure and Applied Geophysics*, *146*, 469-501, 1996.

Sibson, R.H., S.H. White, and B.K. Atkinson, Fault rock distribution and structure within the Alpine Fault Zone: a preliminary account, *Bulletin of the Royal Society of New Zealand*, *18*, 55-65, 1979.

Smith, E.G.C., T. Stern, and B. O'Brien, A seismic velocity profile across the central South Island, New Zealand, from explosion data, *New Zealand Journal of Geology and Geophysics*, *38*, 565-570, 1995.

Stern, T., S. Kleffman, D. Okaya, M. Scherwath, and S. Bannister, Low seismic-wave speeds and enhanced fluid pressure beneath the Southern Alps of New Zealand, *Geology*, *29*, 679-682, 2001.

Sutherland, R., K. Berryman, and R.J. Norris, Quaternary slip rate and geomorphology of the Alpine fault: implications for kinematics and seismic hazard in southwest New Zealand, *Geological Society of America Bulletin*, *118*, 464-474, 2006.

Sutherland, R., and R.J. Norris, Late Quaternary displacement rate, paleoseismicity and geomorphic evolution of the Alpine fault: Evidence from near Hokuri Creek, south Westland, New Zealand, *New Zealand Journal of Geology and Geophysics*, *38*, 419-430, 1995.

Tippett, J.M., and P.J.J. Kamp, Fission track analysis of the Late Cenozoic vertical kinematics of continental Pacific crust, South Island, New Zealand, *Journal of Geophysical Research*, *98*, 16,119-16,148, 1993.

Townend, J., Heat flow through the West Coast, South Island, New Zealand, *New Zealand Journal of Geology and Geophysics*, *42*, 21-31, 1999.

Upton, P., P.O. Koons, and C.P. Chamberlain, Penetration of deformation-driven meteoric water into ductile rocks; isotopic and model observations from the Southern Alps, New Zealand, *New Zealand Journal of Geology and Geophysics*, *38* (4), 535-543, 1995.

Van Avendonk, H.J.A., W.S. Holbrook, D. Okaya, J.K. Austin, F. Davey, and T. Stern, Continental crust under compression; a seismic refraction study of South Island geophysical transect; I, South Island, New Zealand, *Journal of Geophysical Research*, *109* (B6), 16, 2004.

Vry, J.K., A.C. Storkey, and C. Harris, Role of fluids in the metamorphism of the Alpine fault zone, *Journal of Metamorphic Geology*, *19*, 1-11, 2001.

Walcott, R.I., Present tectonics and late Cenozoic evolution of New Zealand, *Geophysical Journal of the Royal Astronomical Society*, *52*, 137-164, 1978.

Walcott, R.I., Plate motion and shear strain rates in the vicinity of the Southern Alps, *Royal Society of New Zealand Bulletin*, *18*, 5-12, 1979.

Walcott, R.I., Modes of oblique compression: late Cenozoic tectonics of the South Island of New Zealand, *Reviews of Geophysics*, *36*, 1-26, 1998.

Wallace, L.M., J. Beavan, R. McCaffrey, K. Berryman, and P. Denys, Balancing the plate motion budget in the South Island, New Zealand, using GPS, geological and seismological data, *Geophysical Journal International*, submitted.

Wallace, R.C., Partial fusion along the Alpine Fault Zone, New Zealand, *Geoligical Society of America Bulletin*, *87*, 1225-1228, 1976.

Wannamaker, P.E., G.R. Jiracek, J.A. Stodt, T.G. Caldwell, V.M. Gonzalez, J.D. McKnight, and A.D. Porter, Fluid generation and pathways beneath an active compressional orogen, the New Zealand Southern Alps, inferred from magnetotelluric data, *Journal of Geophysical Research, B, Solid Earth and Planets*, *107* (6), 22, 2002.

Warr, L.N., and B.A. van der Pluijm, Crystal fractionation in the friction melts of seismic faults (Alpine Fault, New Zealand), *Tectonophysics*, *402*, 111-124, 2005.

Wellman, H.W., Data for the study of Recent and Late Pleistocene faulting in the South Island of New Zealand, *New Zealand Journal of Science and Technology* (B34), 270-288, 1953.

Wellman, H.W., and R.W. Willett, The geology of the west coast from Abut Head to Milford Sound, Part I, *Transactions of the Royal Society of New Zealand*, *71*, 282-306, 1942.

Wells, A., R.P. Duncan, and G.H. Stewart, Forest dynamics in Westland, New Zealand: the importance of large, infrequent earthquake-induced disturbance, *Journal of ecology*, *89*, 1006-1018, 2001.

Wells, A., G.H. Stewart, and R.P. Duncan, Evidence for widespread, synchronous, disturbance-initiated forest establishment in Westland, New Zealand, *Journal of the Royal Society of New Zealand*, *28*, 333-345, 1998.

Wells, A., M.D. Yetton, R.P. Duncan, and G.H. Stewart, Prehistoric dates of the most recent Alpine Fault earthquakes, New Zealand, *Geology*, *27* (11), 995-998, 1999.

Wells, D.L., and K.J. Coppersmith, New empirical relationships among magnitude, rupture length, rupture width, rupture area, and surface displacement, *Bulletin of the Seismological Society of America*, *84* (4), 974-1002, 1994.

Winkler, K.W., and W.F. Murphy, III, Acoustic velocity and attenuation in porous rocks, *AGU Reference Shelf*, *3*, 20-34, 1995.

Wood, P.R., and G.H. Blick, Some results of geodetic fault monitoring in South Island, New Zealand, *Royal Society of New Zealand Bulletin*, *24*, 39-45, 1986.

Wright, C.A., Geology and paleoseismicity of the central Alpine Fault, New Zealand, MSc thesis, University of Otago, Dunedin, New Zealand, 1998.

Yetton, M.D., Progress in understanding the paleoseismicity of the central and northern Alpine Fault, Westland, New Zealand, *New Zealand Journal of Geology and Geophysics*, *41*, 475-483, 1998.

Yetton, M.D., Paleoseismic investigation of the north and west Wairau sections of the Alpine Fault, South Island, New Zealand, *EQC Research Report*, *99/353*, 96, 2002.

Yetton, M.D., A. Wells, and N.J. Traylen, The probabilities and consequences of the next Alpine Fault earthquake, *EQC Research Report*, *95/193*, 1998.

Zachariasen, J., K. Berryman, R.M. Langridge, C. Prentice, M. Rymer, M. Stirling, and P. Villamor, Timing of late Holocene surface rupture on the Wairau Fault, Marlborough, New Zealand, *New Zealand Journal of Geology and Geophysics*, *in press*, 2006.